SINTEF

2017:00835- Unrestricted

Report

A stochastic weather generator based on resampling historical ensemble weather forecasts and its application to hydrological simulation.

Author(s)
Sara Martino
Thomas Nipen, Cristian Lussana, Sjur Kolberg

SINTEF Energy Research AS
Water Resources
2017-12-14

SINTEF

SINTEF Energi AS
SINTEF Energy Research AS

Address:
Postboks 4761 Torgarden
NO-7465 Trondheim
NORWAY
Switchboard: +47 73592000

Enterprise /VAT No:
NO 939 350 675 MVA

KEYWORDS:
Keywords

Report

A stochastic weather generator based on resampling historical ensemble weather forecasts and its application to hydrological

VERSION
1

DATE
2017-12-14

AUTHOR(S)
Sara Martino
Thomas Nipen, Cristian Lussana, Sjur Kolberg

CLIENT(S)
Client(s)

CLIENT'S REF.
Client's reference

PROJECT NO.
502000660

NUMBER OF PAGES/APPENDICES:
32

ABSTRACT

This report presents the *wxgen* weather simulator developed by the Meteorological Institute of Norway and SINTEF energy within the IPN project "Stochastic Weather Generator for Renewable Energy". *wxgen* is a stochastic simulator which creates multivariate synthetic weather series on a grid by resampling the output of a numerical weather prediction model. The ability of *wxgen* to produce realistic weather scenarios depends on the matching algorithm used to join the different weather segments produced by the NWP model and on the characteristics of the database, it resamples from. Here we use a database based on the European Centre of Medium range Forecast re-forecast database. In this report, we describe the main features of the simulator and of the chosen database.

For hydropower industry, the main use of such weather simulator is in hydrological simulation and production planning. We have tested the use of synthetic weather scenarios as input for a hydrological model for a region located in central Norway. The resulting simulated inflow series are then compared to observed ones and to inflow series simulated with historical weather as input for the hydrological model.

PREPARED BY Sara Martino	SIGNATURE Sara Martino
CHECKED BY Sjur Kolberg	SIGNATURE Sjur Kolberg
APPROVED BY Julie Charmasson	SIGNATURE

REPORT NO.	**ISBN**	**CLASSIFICATION**	**CLASSIFICATION THIS PAGE**
2017:00835	ISBN	Unrestricted	Unrestricted

A stochastic weather generator based on resampling historical ensemble weather forecasts and its application to hydrological simulation.

Sara Martino, Thomas Nipen, Cristian Lussana, Sjur Kolberg

December 14, 2017

Contents

1 Introduction

Stochastic weather generators (SWGs) aim to generate synthetic weather sequences with statistical properties that resemble real weather sequences. These synthetic sequences can be used in place of observational records, which often are incomplete and limited in spatial and temporal extent. Although SWGs are based on finite amount of input data, they allow an arbitrary number of arbitrarily long sequences to be made.

End uses of such weather sequences are numerous. We focus here on energy production planning and hydrology where information about the risks of various weather sequences is needed.

The weather sequences generated by a WG, in order to be useful, need to be realistic in their spatio-temporal pattern but also they need to respect the correct dependence structure in space, in time and between the different weather variables.

Traditionally, SWGs are built by statistically modeling the relationships between variables of interest in space and time. Wilks and Wilby (1999) provides an extensive summary of this approach. These generators can create any desired number of sequences cheaply by sampling sequences from the statistical model. The models are designed and fitted using available observations. A challenge with constructing such statistical models is ensuring that the correlations in time, space, and across variables are realistic. While creating models that perform well for a single variable and location can be straight forward, the complexity increases immensely when this is expanded to multiple variables and in space.

An alternative approach to SWGs is to use a physics-based climate model to simulate weather conditions in the atmosphere forward in time. A set of realization can be obtained by using different initial conditions or by cutting long multi-year scenarios into one-year scenarios. This procedure requires vast amount of computing power to get a sufficiently large set of realization at a high enough resolution.

We present a hybrid approach to weather generation by stochastically resampling output from numerical weather prediction (NWP) models. A working prototype of this hybrid simulator is called the *wxgen* weather simulator and is available for users to test. The *wxgen* weather simulator creates arbitrarily long, multivariate time series of weather variable on a grid by joining together weather segments produced by a NWP model.

For hydro-power companies the final use of the weather sequences produced by a WG is in hydrological modeling. The aim is to substitute historical weather sequences with simulated ones. In this report we have tested one simulated weather scenario in a hydrological model for a region located in central Norway. The resulting simulated inflow series are compared with observed ones and with inflow series simulated using historical weather as input for the hydrological model.

The report is organized as follows: Section provides a brief summary of the weather generator under evaluation and of the database it resamples from. For a more extensive description, see Nipen et al. (2017). Section 3 describes the case study for testing the use of simulated weather scenarios in hydrological simulation. We describe the region chosen, the hydrological model and the three series of weather variables which have been used as input to simulate inflow series, namely the observed weather, the day zero forecast from the EC numerical weather prediction model and the *wxgen* simulated weather series. Section 4 compares the inflow series simulated from the hydrological model with the different weather input. We end with a discussion in Section 5.

2 The *wxgen* simulator

The *wxgen* simulator is a weather generator which creates multi-variable, synthetic weather sequences over an arbitrary spatial domain, by stochastically resampling output from numerical weather prediction (NWP) models, Nipen et al. (2017). A prototype of the simulator can be downloaded from `https://github.com/metno/wxgen`, a wiki page provides also guidelines and a tutorial on how to use it.

The resampling approach used in *wxgen* leverages the many weather prediction scenarios that have been and are currently being made operationally. In particular, the European Centre for Medium Range Weather Forecast (ECMWF)'s ensemble prediction system provides a large number of historical weather sequences that can be stochastically joined together into longer timeseries. In this study, we have considered the dataset of medium-range ensemble reforecast, ENS-refc (Buizza and Leutbecher, 2015; Vitart and Coauthors, 2017), and specifically we have used 10-day weather sequences for the joining.

Compared to weather generators built by statistically modeling the relationships between variables of interest in space and time (see for example Wilks and Wilby (1999) for an extensive review), the resampling method offer some advantages: Firstly, correlations in space and across variables are forced to be consistent with the physical reality as described by the NWP model. Also, the generator does not need to statistically model the transitions from one time to the next, as the NWP model simulates this. Secondly, extending the generator to other variables does not require extensive statistical modeling, provided the requested variables are available in the NWP model. Thirdly, end users do not need to maintain a database of observation series. This is especially an advantage when a trans-national domain is desired where acquiring and processing observations from several institutes is time consuming.

On the other side, a matching algorithm is needed to join two 10-day weather segments. The method that ensures continuity beyond the 10 days is the core of this type of weather generator. Also, resampling methods cannot generate events that have not been observed historically. While this is true on a daily timescale in this application, the generator can still create extreme weekly or monthly events.

In the Section 2.1 we briefly review how the 10-days weather sequences are joined in *wxgen* to generate longer weather scenarios.

The spatio-temporal characteristics of the *wxgen*-simulated weather sequences are highly dependent on the characteristic of the NWP database we resample from. If a bias is present in the NWP model we will find it also in the simulated scenarios. For this reason, in Section 2.2 we describe more in detail the database we used in this study and compare it to observed weather data to check possible biases.

2.1 Joining Sequences

Joining segments is the key part of the *wxgen* weather generator. If segments were joined randomly it would result in a time series with unrealistic jumps at the transition from one segment to the other.

In general we want the end state of one segment to mach as closely as possible the starting state of the next one, see Figure 1. To achieve this, a metric must be chosen for the comparison. The weight root mean squared difference is commonly used in analog approaches (Delle Monache et al., 2011). This metric can compare one or several weather variables. Because weather variables have different measuring units, weights have to be

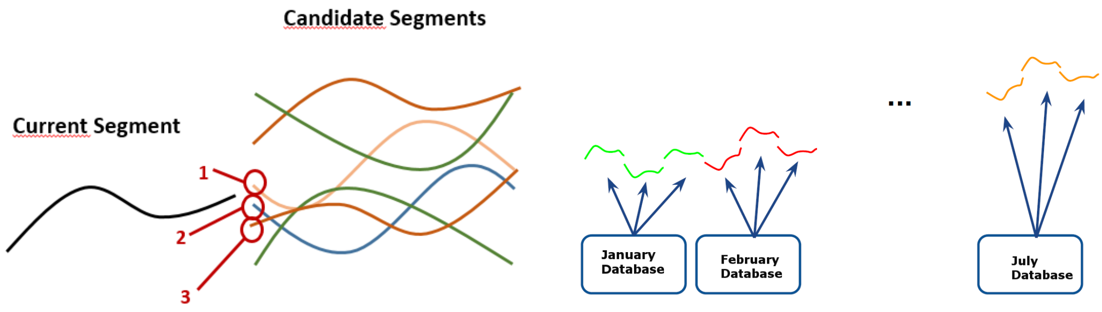

a) b)

Figure 1: a) Within the 10-day segments, the sequence is dictated by the atmospheric model. Between segments, we want the end state of one segment to mach as closely as possible the starting state of the next one. A metric is computed for each candidate segment and one of the best n candidates is randomly selected. b) A representation of the seasonal databases.

introduced to scale the variables and to regulate the relative importance of each variable to the total value of the metric.

The metric can be computed using aggregated values over the whole domain, for example the spatial mean temperature of the last day of one sequence can be compared to the spatial mean of the first day of the next sequence. Alternatively one could try to match the weather variables more locally, for example using wavelets as will be discussed later on.

The metric we use has the following form: for the current segment $\mathbf{y}$, for each candidate segment $\mathbf{x}$ in the relevant database

$$S_{\mathbf{yx}} = \sum_{\nu=1}^{k} w_\nu \ \mathrm{RMSD}\big(f(y_\nu^{10}), f(x_\nu^1)\big) \tag{1}$$

Where

- k is the number of weather variables that are included in the score (for example temperature and sea level pressure)
- w_ν is a weight (it also depends on the measuring units of the variable)
- y^{10} and x^1 indicates the 10th day in the current segment and the first day in the candidate segment
- RMSD$(\cdot)$ is the root mean squared difference
- $f(\cdot)$ is a functional of the relevant map (for example the aggregated value over the whole domain)

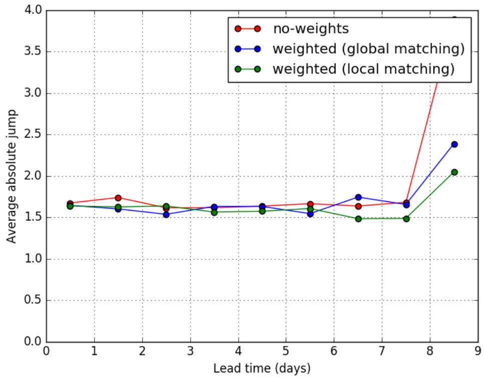

Figure 2: Average absolute difference between two successive states in one grid node. Lead time 1-8 refer to consecutive days within the same segment, while lead time 9 refers to consecutive days that span two segments. In red are the scores for a simulation without any metric, in blue is a simulation with metric with global spatial matching (areal average) and in green is a simulation with local spatial matching (wavelets).

After scoring all candidate segments, the next step is to elaborate a policy for selecting one of the candidates. The obvious approach would be to chose the segment with the best score, that is the one whose first day that best matches the last day of the previous one. One severe drawback of such approach is that it would create loops in the simulated timeseries as a given end state will always be connected with the same segment. To add stochasticity, a random selection of the candidate segments can be made, while at the same time accounting for the score assigned to the segments. Our choice was to randomly select one the of n best candidates.

Figure 2 shows that the introduction of a metric in the resampling algorithm reduces the jumps at the transition from one segment to the other. The average absolute difference between two successive states has been computed for different times. Ideally, the difference, on average, should be the same between two consecutive days between two consecutive days in different segments. In Figure 2 lead time 1-8 refer to consecutive days within the same segment, while lead time 9 refers to consecutive days that span two segments. When a weighted metric is introduced, the mean difference between two consecutive days that span two segments drops significantly.

Even after establishing a metric , joining segments into one-year sequence does not guarantee that the simulated sequence exhibits seasonal characteristics. For example, nothing prevents a November sequence to be joined to a January one. To ensure a realistic seasonal signal, the dataset has been separated into seasonal databases that are sampled in order, see Figure 1.

An alternative to aggregating values over the whole domain when computing the metric in equation 1, is to use wavelet decomposition to allow for a more local matching. Spatial matching using wavelets reduces jumps at the local scale, see Figure 2.

A common problem with stochastic weather generators is their inability to have large enough long-term variance (Wilks and Wilby, 1999). Our hybrid approach can also exhibit this problem. This is caused by the fact that information about slow-varying states are not represented in the states of the segments. This means that for example, an extended warm summer are less likely to be represented in the ensemble of trajectories. One way to improve the situation, is to connect two 15 day segments from the same year together before they are selected. That is, the database can pre-join the segments into 30-day or 45-day segments. This partly captures latent states that cause a segments to stay warmer, colder, dryer, or wetter for prolonged periods of times.

In short, when simulating weather scenarios with *wxgen* the user meets the following choices:

- Which variables to include in the metric in equation 1
- Which weight to give to each variable in the metric in equation 1
- Which spatial resolution to choose
- Whether to pre-join the segments or not

Some guidelines for the users regarding this choices are given in the wiki page of the *wxgen* project (`https://github.com/metno/wxgen/wiki`).

2.2 The EC database

The database used in this study, is based on ENS-refc dataset of reforecasts. Reforecasts have been initially introduced in NWP practice by Hamill and Coauthors (2014) and a review of their use within ECMWF is reported by Gneiting (2014): "Reforecasts are retrospective weather forecasts, where todays NWP models are applied to past initialization and prediction dates. As the reforecasts are based on the model version that is currently run operationally, the availability of reforecast datasets can result in massive enlargements of training sets for statistical postprocessing.'.

According to the user guide to ECMWF forecast products (version 1.2, available at `https://www.ecmwf.int/files/user-guide-ecmwf-forecast-products`), since May 2015 ECMWF reruns today's operational model for past dates in ENS-refc.

Twice a week, the operational model is rerun for the same day of year for the previous 20 years. That is, on Jan 15 2016, the operational model is rerun for 15 days starting on Jan 15 for each of the years between 1997 to 2015.

This dataset samples a much richer climatology than the operational dataset of forecasts for a single year and ENS-refc is actually used to provide a reliable model climate. Having a richer climatology to sample from allows the joins to match better. As the model is constantly upgraded, the scenarios on the dataset can vary though always including sequences of possible weather.

Our database contains 10-days long reforecasted weather sequences on a 0.25° by 0.25° grid. It includes daily averages of 2 m air temperature, 10 m zonal winds, 10 m meridional winds, cloud coverage, and daily totals of precipitation. Moreover, solar

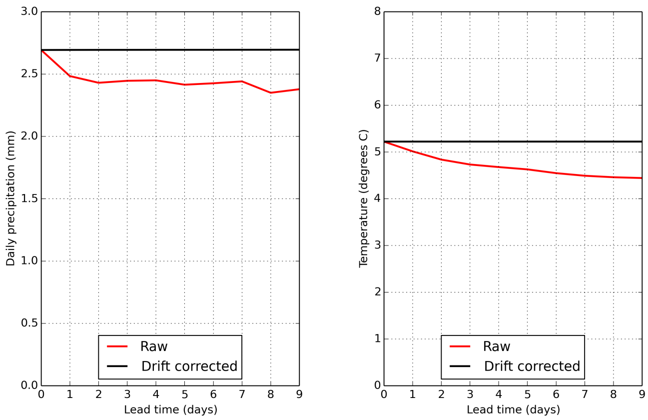

a) b)

Figure 3: Average daily temperature (a) and daily precipitation (b) for the ECMWF hindcasts for the 60^o N, 10^o gridpoint. Both the raw forecast and the drift-corrected forecasts using quantile-mapping towards leadtime 0.

radiation is computed from the cloud coverage and the time of the year. This set of variables is suitable for hydrological applications and energy production planning. In addition it includes sea level pressure. Although this variable is not of direct interest of the user, its large scale pattern will aid in joining segments together. The spatial domain is limited to the south of Norway, mostly to reduce the memory usage.

Weather models often exhibit a tendency to drift over time. This occurs when the model has a different climatology than the climate imposed by data assimilation. The drift was corrected by applying a quantile mapping between each lead time and the first lead time (Fig. 3). This was done independently for each gridpoint for both temperature and precipitation.

In the rest of the report, we indicate the selected subset of the ENS-refc dataset that is used as basis for the *wxgen* simulator as EC database.

To check possible biases in EC database, we compare the day 0 forecast from the hindcast with observed weather data. We do this for temperature and precipitation. The day 0 forecast is the closest we come to historically observed weather. As observed data we use daily temperature and precipitation maps from the seNorge2 database. This are high resolution (1×1 Km) interpolation maps for temperature and precipitation created by the Meteorological Institute of Norway, see Lussana et al. (2017b) and Lussana et al. (2017a) for details on how such maps are created. For comparability, the high resolution maps have been up-scaled to the same spatial resolution as the EC database.

The difference in mean temperature between the observed and the EC database (computed over the whole period 2005-2015) is represented as a function of spatial location and altitude in Figure 4a) and 4b), and as a function of julian day in in Figure 4d). There is a clear tendency of the EC database to underestimate the mean temperature in the mountainous areas (4a). A altitude gradient is also clearly present in Figure 4b). The difference in mean temperature has also a seasonal component. It tends to be higher in winter and lower in summer. In the winter period the EC dataset underestimates temperatures. Figure 5 shows that there is actually an interaction between the spatial and the temporal bias. Figure 5 displays the mean difference in temperature as function of the spatial location for the four season: Spring (March-May), Summer (June-August), Autumn (September-November) and Winter (December-February). In the summer there is relatively small difference between the two datasets. The difference is larger in winter for the mountainous areas but is present also in Spring and Autumn, also then stronger in the mountains. This bias in temperature could have large impact on the hydrological model. Lower temperatures in Winter, Spring and Autumn mean longer and and colder winters with less activity in the catchments and larger spring floods.

Figure 6a) and 6b) shows the mean difference in precipitations as function of spatial location and altitude. The EC dataset tends to underestimate precipitation on the coast (especially the south-east coast) and overestimate it on the mountains. There is a slight altitude gradient in the bias (Figure 6b)). On the other side, Figures 6c) and 6d) seem to exclude a seasonal bias in the representation of precipitation of the EC database. There seems so be, on average, an overestimation through the whole year.

3 The case study for hydrological simulation

3.1 The region

To test the use of *wxgen* simulated weather series in hydrological simulation we have selected a region in central Norway of approximately 190 $\times$ 230 kilometers. Altitude goes from 0 to 2300 m above sea level with an average of 1019 meters. In this area we have 45 observed inflow series. The area and the location of the observed inflow series are represented in Figure 7. Names, NVE series number and size of catchment area (in km^2) for each series are reported in Table 1 Most of the series in this region have a typical mountain inflow regime, with little activity in the winter period and spring flood.

3.2 The hydrological model

The hydrological simulations were conducted using the Enki framework for distributed modelling. The selected model was composed of the GamSnow energy-sum snow routine, the Priestley-Taylor method for potential evapotransporation, the KirchnerMod response routine and the basic QSubcat catchment aggregator. For runs with measured input, the complete model also included interpolators for radiation and wind speed. Documentation of the Enki framework and the involved routines are provided in Kolberg and Saether (2017) and references herein.

The model was calibrated regionally using 45 catchments listed in Table 2, on daily data for the period 1999-2003. Precipitation and temperature maps with 1 km resolution for the same period are taken from the seNorge2 database (Lussana et al., 2017a,b).

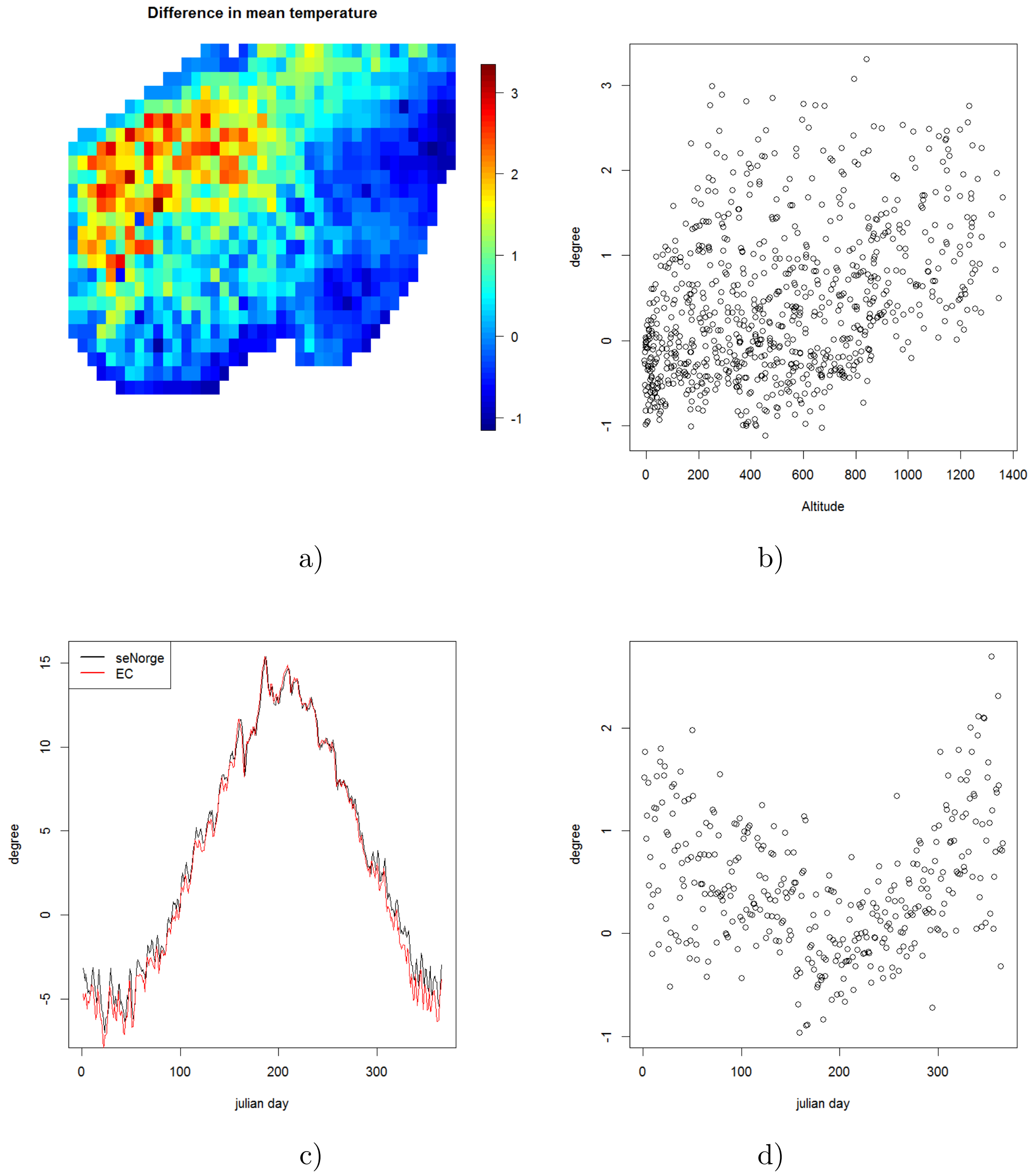

Figure 4: a) Difference in mean temperature between observed and EC dataset as function of spatial location. b) same difference plotted against altitude. c) Mean yearly temperature profile over the whole domain as observed (black) and from the EC dataset (red). d) Difference in mean temperature as function of julian day.

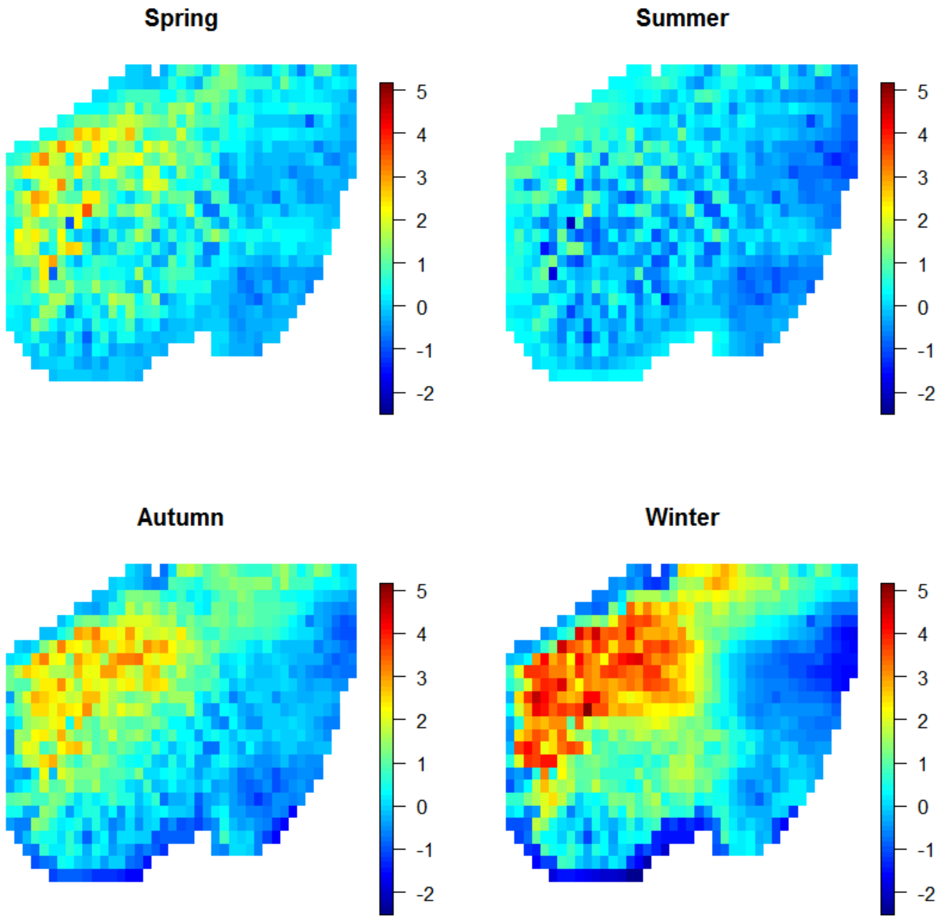

Figure 5: Difference in mean temperature between observed and EC dataset as function of spatial location in the four seasons.

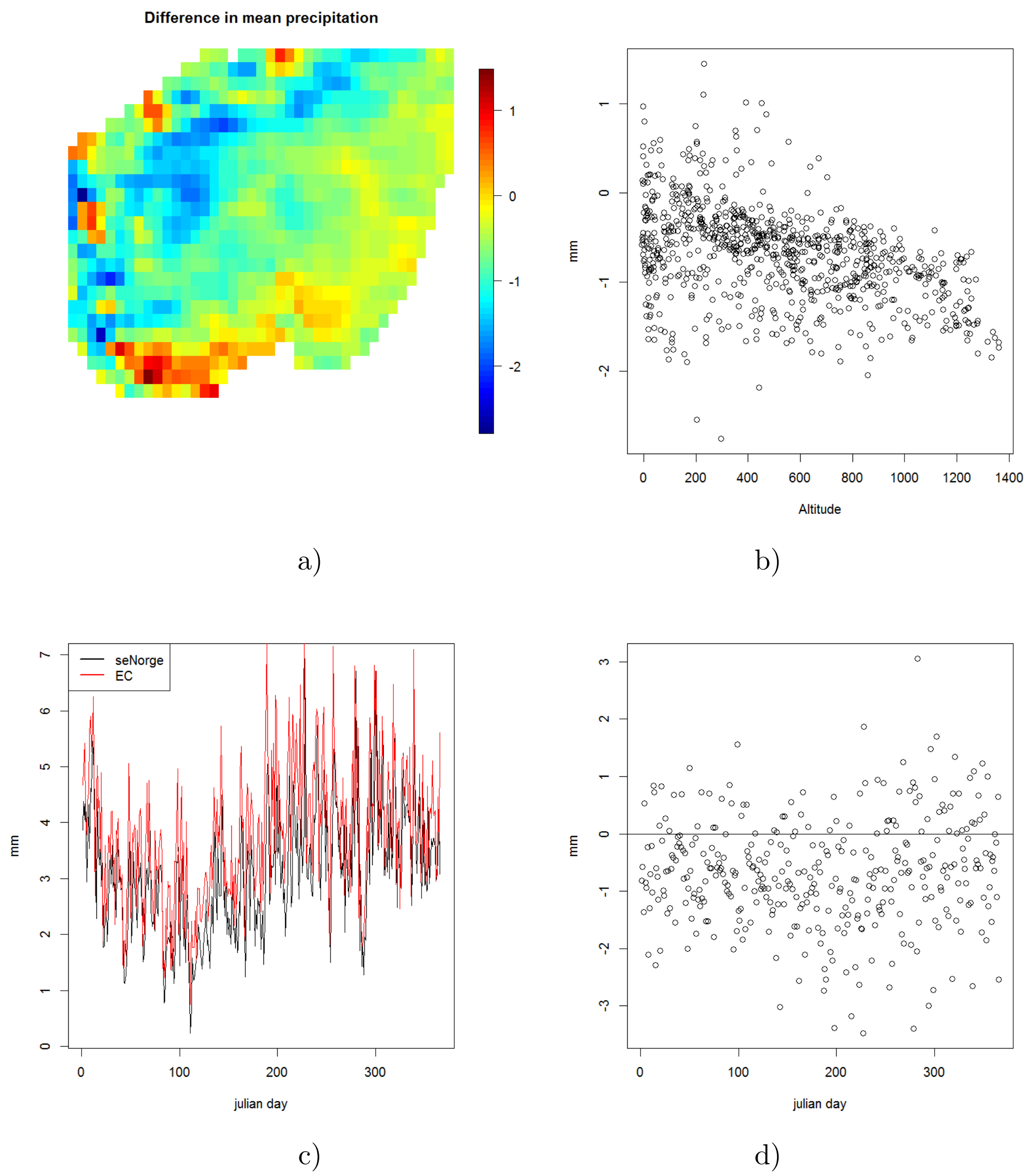

Figure 6: a) Difference in mean precipitation between observed and EC dataset as function of spatial location. b) same difference plotted against altitude. c) Mean yearly precipitation profile over the whole domain as observed (black) and from the EC dataset (red). d) Difference in mean temperature as function of julian day.

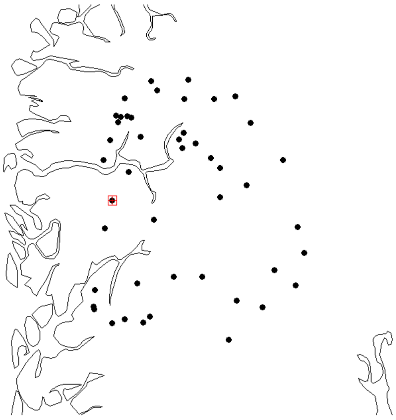

Figure 7: Selected region with the location of the 46 observed inflow series. The red square indicates the position of the Myrkdalsvatn station.

Maps for radiation and wind are constructed by interpolation of data from the NIBIO observation network. Available data for relative humidity were replaced by a fixed value of 80 %, to maximise similarity with the EC database used in further analyses. The calibration reached an average Nash-Sutcliffe efficiency of 0.55. Better performance can be expected for a smaller set of carefully monitored catchments, and for catchment-specific calibration. For this project's task of evaluating the effect of using varying input, the performance was considered sufficient, and a more thorough analysis of errors was not performed. The list of parameters and their values (optimised or a priori set) is given in table 2.

3.3 Input to the hydrological model

The chosen hydrological model needs the following weather variables as input: humidity, wind velocity, precipitation, temperature and solar radiation. Humidity is not part of the EC database, therefore for all simulations, humidity is set to be constant over time and space to 80%.

In this section we describe the three sets of weather scenarios we have used as input to the hydrological model.

3.3.1 Observed weather (seNorge weather)

The first input series consists of observed weather. The observations cover the period 2005-2015.

For temperature and precipitation we used the daily seNorge2 maps. Maps for wind and solar radiation are obtained by kriging interpolation of daily observed quantities from the NIBIO net. The location of the observation stations are displayed in Figure 8.

Figure 8 shows the mean field over the period 2005-2015 for the four weather variables. In the rest of the report we denote this series of weather variables as seNorge weather.

3.3.2 EC weather

The second weather series consists of the day 0 forecast in the EC database from 2005 to 2015. This is what we define as “truth” in the *wxgen* context.

Temperature is downscaled to 1×1 km grid by using a altitude gradient of -0.6 $^{o}C/100$ m, constant over time and space. Precipitation is downscaled to 6×6 km grid using quantile-quantile mapping. The quantile-quantile maps is constructed by comparing the day 0 forecast database to the COSMO regional reanalysis dataset (`http://reanalysis.meteo.uni-bonn.de}`)which has a spatial resolution of 6 kilometers. The other weather variables (wind and solar radiation) are not downscaled and used in their original scale.

Note that our downscaling procedure corrects some of the bias for precipitation but not for temperature. In the following the show plots for the downscaled fields where downscaling apply.

Figure 10 shows the mean field over the period 2005-2015 for the four weather variables. Comparing Figure 10 with Figure 8 it is clear that while temperature and precipitation show roughly the same features, wind and solar radiation are very different. These differences can depend on several factors: the location of the observation net could be one of these. Moreover, the NIBIO wind is observed at 2 meters height while wind in the EC database refers to 10 m height.

We look more in detail to the temperature variable. Figure 9 (left side) compares the yearly EC and seNorge temperature profile, averaged over the area of interest. This is similar to Figure 4c) but only for the area selected for hydrological simulation. The EC data set presents, on average, lower temperatures from May to November and (on average) slightly higher temperature in the rest of the year. The right side of Figure 9 displays the estimated probability of temperature beling below zero for the two data sets. The EC data set presents a higher probability of temperature being below zero both the in the spring and autumn period. This affects, of course, the outcome of precipitation as snow or rain and, as a consequence, the regime of the inflow series.

In the rest of the report we denote this series of weather variables as EC weather.

3.3.3 WX weather

The last weather series is simulated from the large scale weather generator *wxgen*. We simulate a 10 years long weather series using the following *wxgen* command line:

wxgen sim -db ECdatabase.nc -v 0,1,2,4,5,6 -w 100000,0,1,0,0,0 -wl 3 -n 1 -t 4015 -o sim10years.nc

That is we use the large scale variables temperature and sea level pressure to compute the metric in Equation 1. Moreover, we use level 3 wavelets decomposition for the spatial

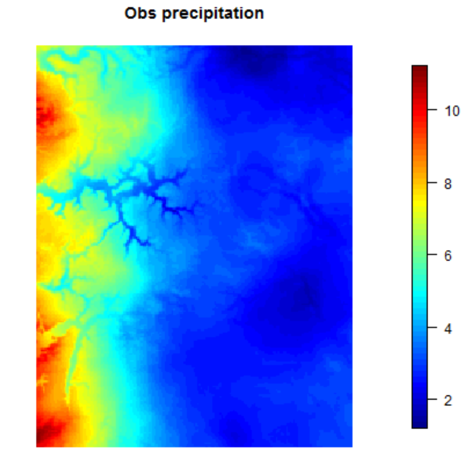

a) Precipitation

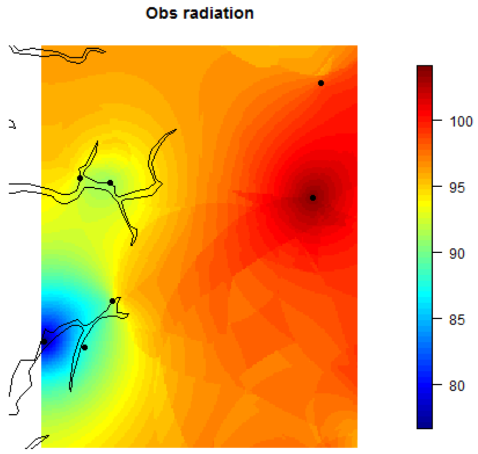

b) Solar radiation

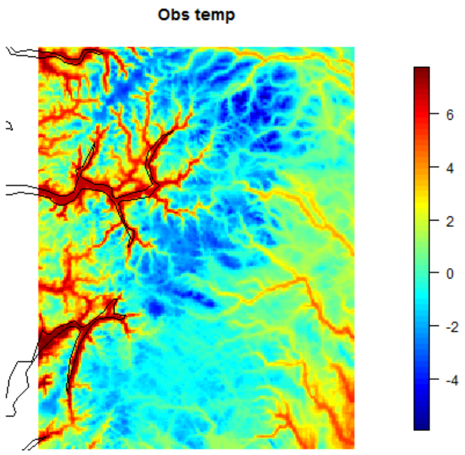

c) Temperature

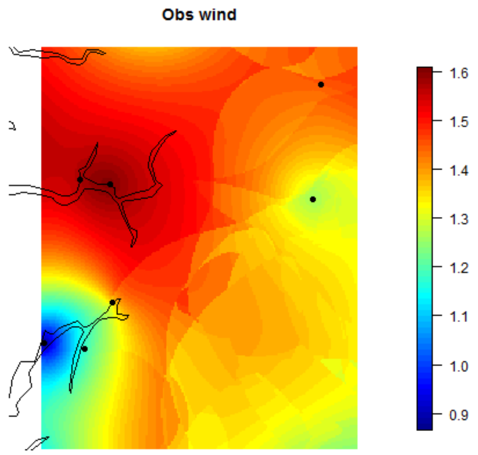

d) Wind speed

Figure 8: Mean spatial field for a) precipitation b) solar radiation c) temperature and d) wind speed for the seNorge weather series. The black dots in b) and d) indicate the location of the observation stations of the NIBIO network.

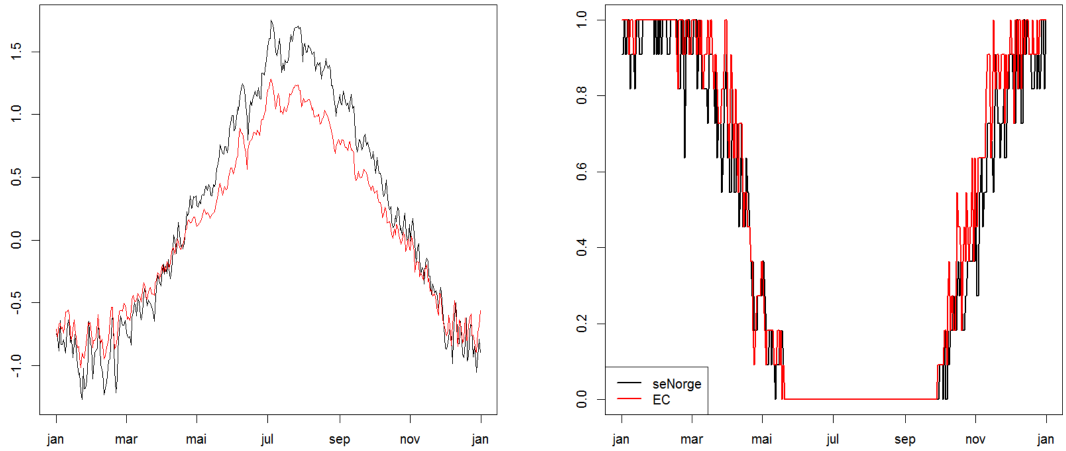

Figure 9: Domain averaged yearly temperature profile (left) for the seNorge and EC dataset. Domain averaged probability of temperature being below zero (right).

matching. Table 3 explains the meaning of the various options used in the call to *wxgen*. For more information on how to run the simulator and a description of all possible options see the wiki page of the project `https://github.com/metno/wxgen`.

Figure 11 compares the jump statistics, for one random grid cells, between the simulated weather series and the day 0 EC forecast (the "truth"). The results are quite good, in the sense that there appears to be no big difference between two consecutive days that are within one segment (lead times 1 to 8 in the Figure 11) and two consecutive days that span two segments (lead time 9 in the Figure 11).

Notice that although we only included temperature and sea level pressure in the score in equation 1, we get smooth series also for the other variables.

Figure 12 compares the variance (for one random grid cell) aggregated over different time scales. All four weather variables are displayed. It is known that the *wxgen* simulator tends to underestimate the variance aggregated over long time scales. This is visible also in Figure 12 especially for the temperature variable.

The simulated time series has, of course, the same spatial resolution as the EC series. The downscaling for this weather series is similar to the one used for the EC weather series.

Figure 13 shows the mean field over the period 2005-2015 for the four weather variables. The plots are quite similar to the ones in Figure 10.

We indicate the weather time series simulated through *wxgen* as WX weather.

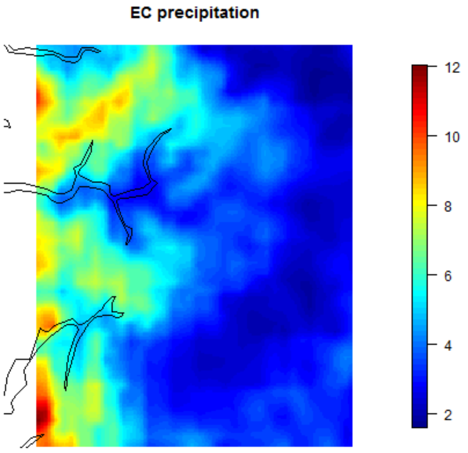

a) Precipitation

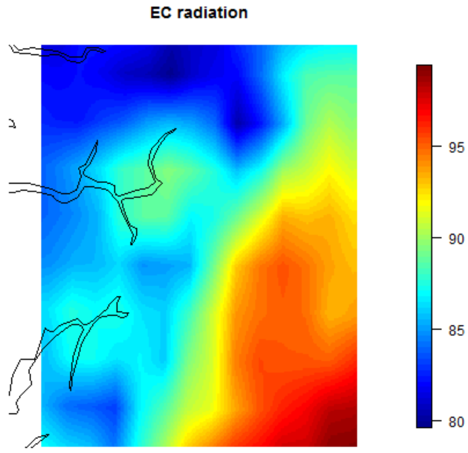

b) Solar radiation

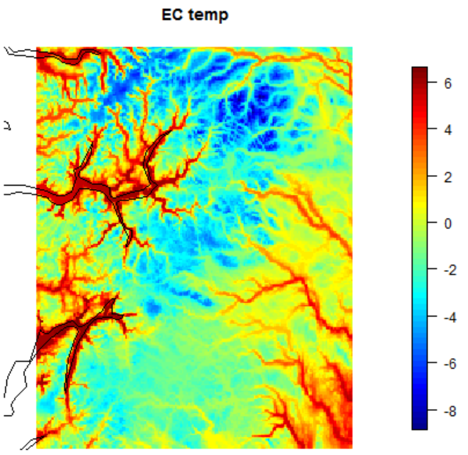

c) Temperature

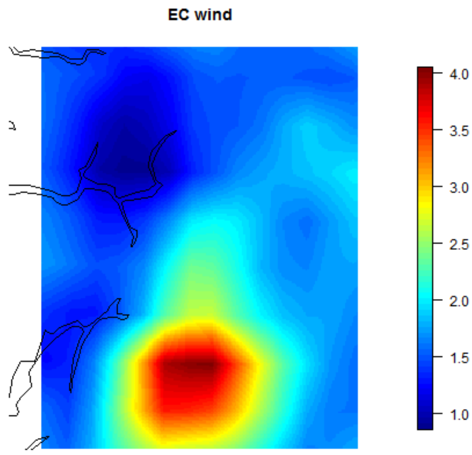

d) Wind speed

Figure 10: Mean spatial field for a) precipitation b) solar radiation c) temperature and d) wind speed for the EC weather series.

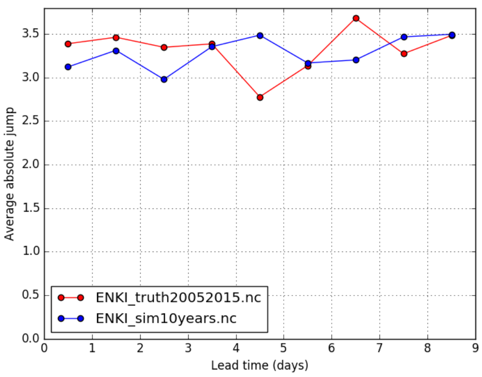

a) Precipitation

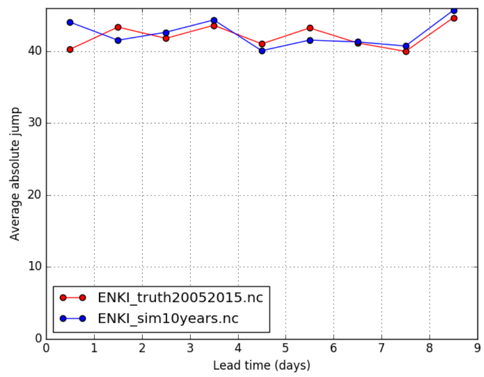

b) Solar radiation

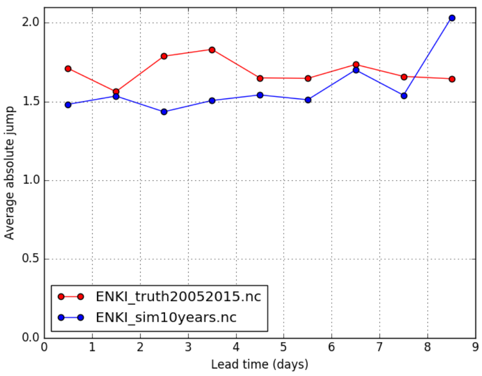

c) Temperature

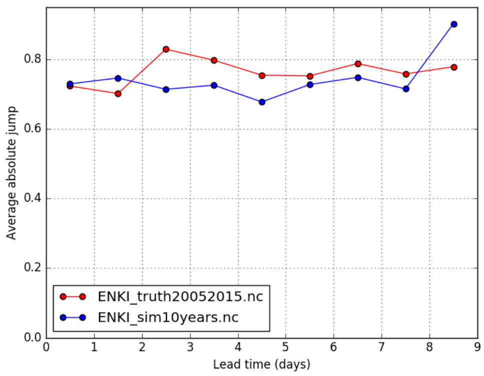

d) Wind speed

Figure 11: Jump statistics, for one random grid cells, for the four simulated weather variables.

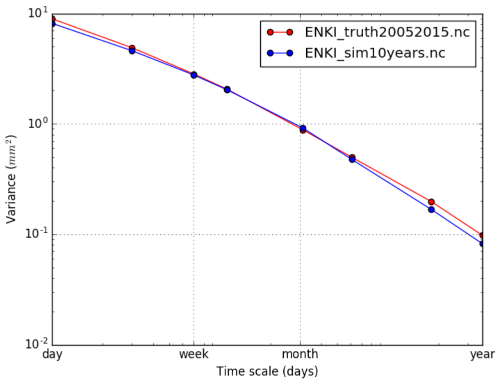

a) Precipitation

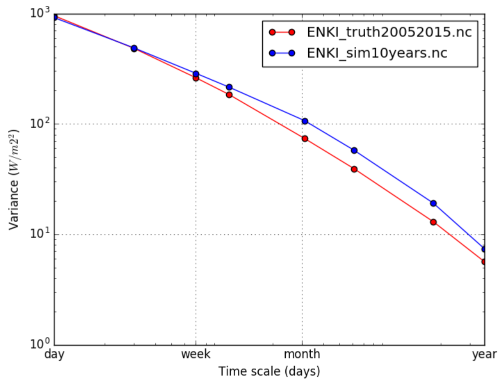

b) Solar radiation

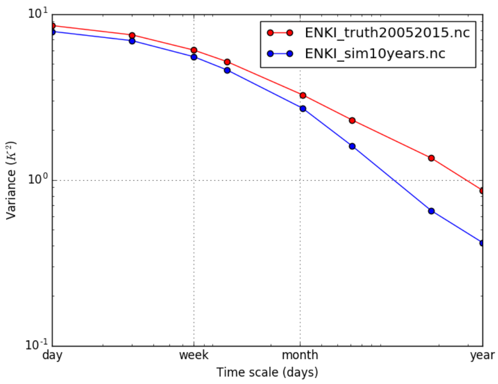

c) Temperature

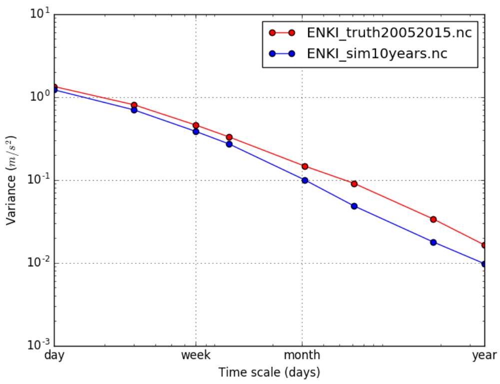

d) Wind speed

Figure 12: Comparison of variance for one random grid cell, aggregated over different time scales, between the EC weather series (red line) and the WX weather series (black line) for the four weather variables used to drove the hydrological model

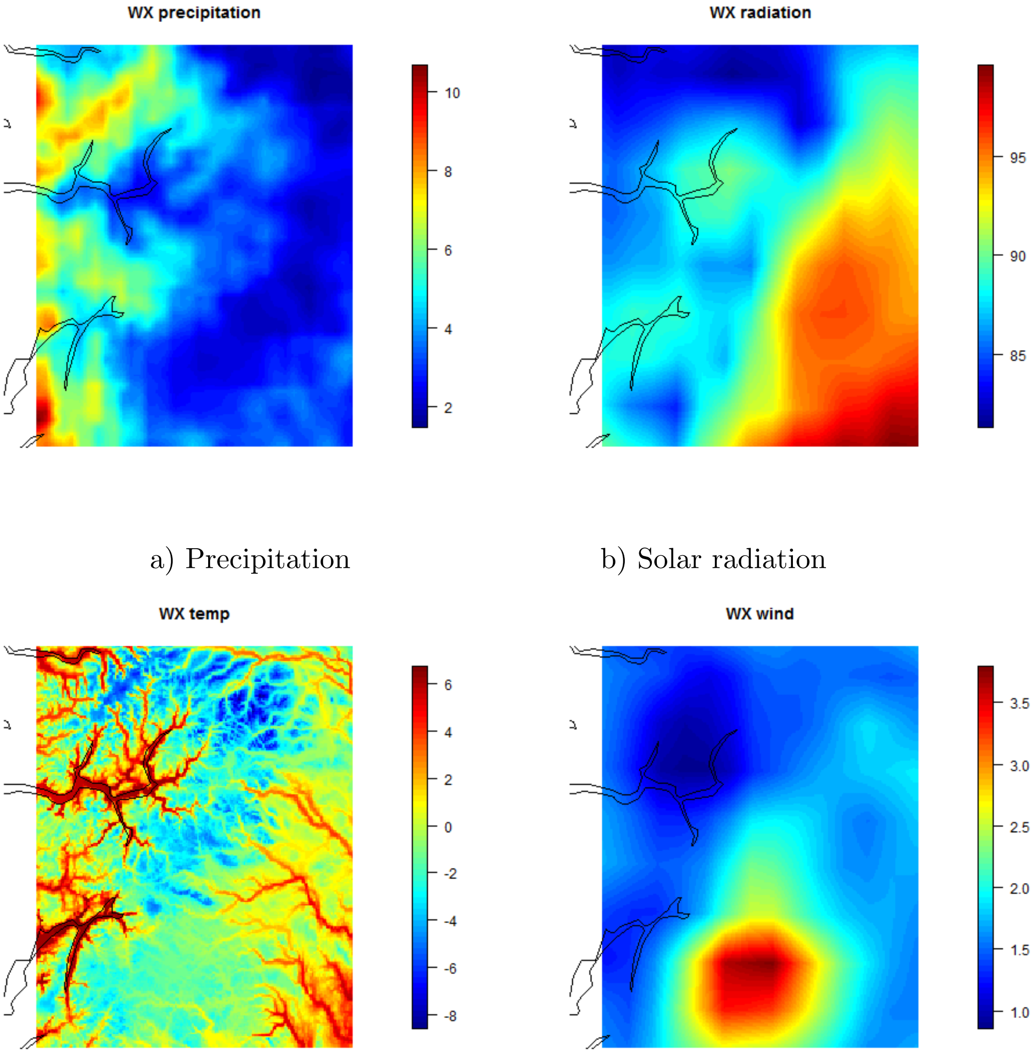

a) Precipitation

b) Solar radiation

c) Temperature

d) Wind speed

Figure 13: Mean spatial field for a) precipitation b) solar radiation c) temperature and d) wind speed for the WX weather series.

4 Results

We ran the hydrological model using our three different weather series as input.

The parameters of the hydrological model are kept constant in the three simulations and are those reported in Table 2. To account for the difference between observed and EC wind fields observed in Sections and we have used the ratio between mean observed and mean EC wind to scale the WindScale1 parameter of the GamSnow energy-sum snow routine in Table 2 over the domain.

We obtain three different sets of inflow series:

- The inflow series simulated when the hydrological model is fed using the seNorge weather, we indicate this set of inflow series as seNorge inflow series
- The inflow series simulated when the hydrological model is fed using the EC weather, we indicate this set of inflow series as EC inflow series
- The inflow series simulated when the hydrological model is fed using the WX weather, we indicate this set of inflow series as WX inflow series

In addition we have the observed inflow series which we indicate as WX inflow series OBS.

In Figure 14 we have plotted the mean observed inflow for each catchment against the mean simulated seNorge inflow (left column), EC inflow (center column) and WX inflow (right column). The EC and WX inflow series seems to replicate quite well the annual mean inflow and to slightly overestimate the spring inflow. There is a clear underestimation of the winter inflow. This is true also the the seNorge inflow but to a much smaller extent.

When comparing the three sets of simulated inflow series with the observed one, the largest difference we observe is that the simulated series have a more extreme mountainous regime, with less activity in the winter months and larger spring floods than the observed inflow series.

This feature is present for all the three simulated inflow series but more pronounced for the EC and WX series. Figure 15 shows the ratio between the mean winter inflow (months from December to February) and the mean spring flood (months from April to June) for all the 45 inflow series under study. With a couple of exception this ratio is much more extreme for the observed and seNorge series than for the EC and WX series. We can also notice that the EC and WX series have a quite similar behavior.

To understand where this difference comes from we look in more detail to some of the 45 series. Figure 16 shows the inflow for the Myrkdalsvatn catchment. The location of this catchment is indicated in Figure 7. On the left side of Figure 16 is the yearly profile for the inflow. The EC and the WX series have clearly less activity during the winter months. Also, the peak spring flood appears to arrive later and be larger for these series than for the OBS and seNorge series. We found the same kind of behavior for several of the series in this study.

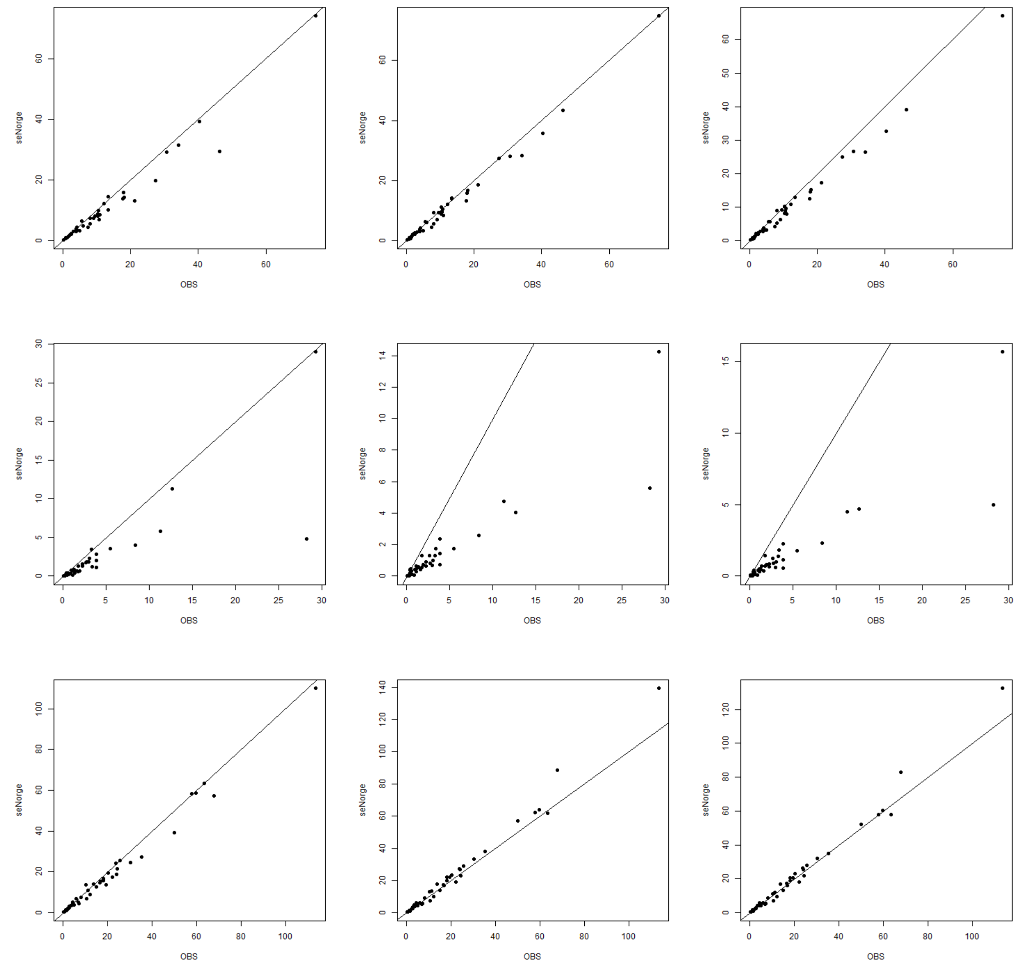

Figure 14: Observed mean inflow plotted against seNorge mean inflow (left column), EC mean inflow (center column) and WX mean inflow (right columns). The upper line refer to the whole year, the center line to the winter season (months from December to February), the lower row to the Spring season (months from April to June).

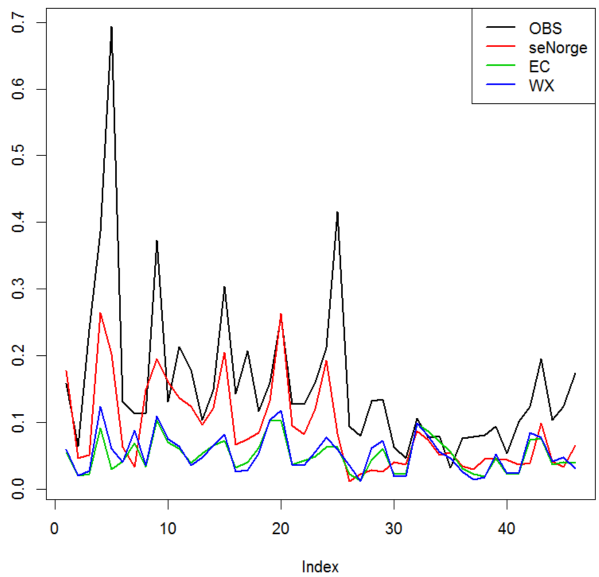

Figure 15: Ratio between mean winter Inflow (December-February) and mean spring inflow (April-June) for the 45 inflow series in study. The observed series are plotted in black, the seNorge series in red, the EC series in green and the WX series in blue.

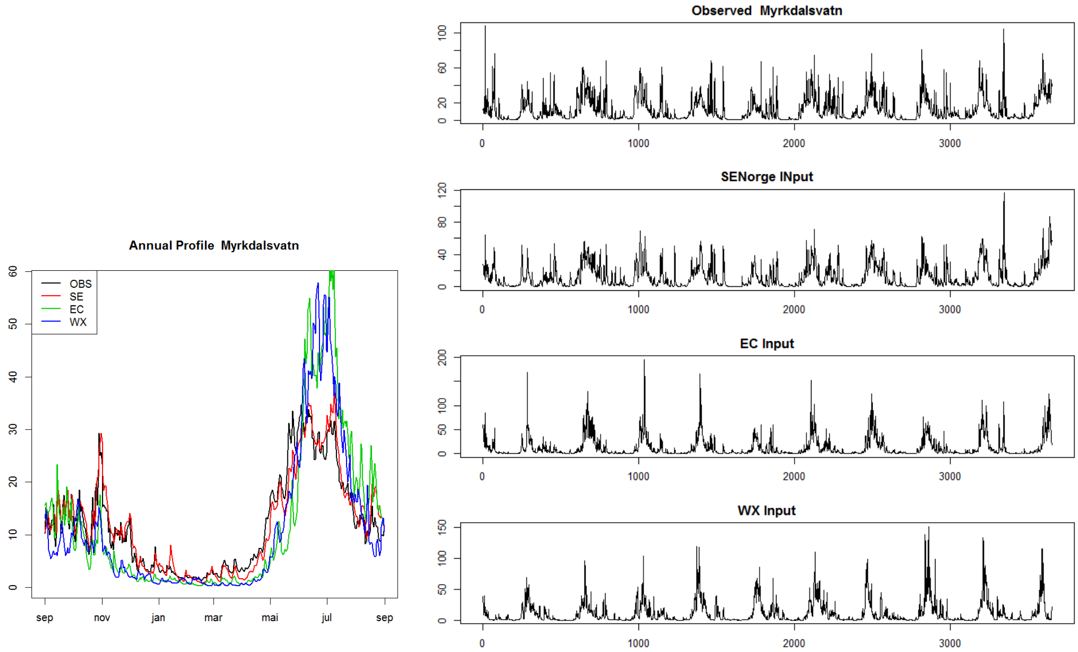

Figure 16: Inflow at the Myrkdalsvatn station: yearly profile (left side) and hydrogram (right side). The observed and all three simulated inflow series are represented

Figure 17 shows the yearly profile for the weather variables (temperature, solar radiation, wind and precipitation) averaged over the Myrkdalsvatn catchment. While for solar radiation, wind and precipitation the seNorge data are in agreement with both the EC and the WX data, for temperature we observe that on average seNorge winters are milder and shorter. This is also observed over several of the catchments in this study.

We have already observed in Section 3.3.2 that the EC temperature tend to have, on average, higher probability of being below zero for both the spring and the autumn season and that this feature would affect the regime of the simulated hydrological series.

In addition, to downscale the EC and WX temperature fields, we have used a fixed altitude gradient over the whole domain without accounting for any seasonality. To check the possible presence of a seasonality in the altitude gradient we have estimated it from the seNorge dataset. The result is displayed as a black line in Figure 18. The seasonal cycles is evident. In red, in the same Figure, is the altitude gradient estimated from the downscaled EC dataset. The (less evident) seasonal cycles comes from the EC data set. Probably a better estimate of the altitude model and/or a bias correction of the EC temperature could have make the EC and WX inflow series more similar to the observed and seNorge ones.

We look now at the spatial correlation between the inflow series. Figure 19 shows the correlation matrix for the 46 stations. The correlation has been computed considering the daily values for the whole year after subtracting the mean yearly profile. In the

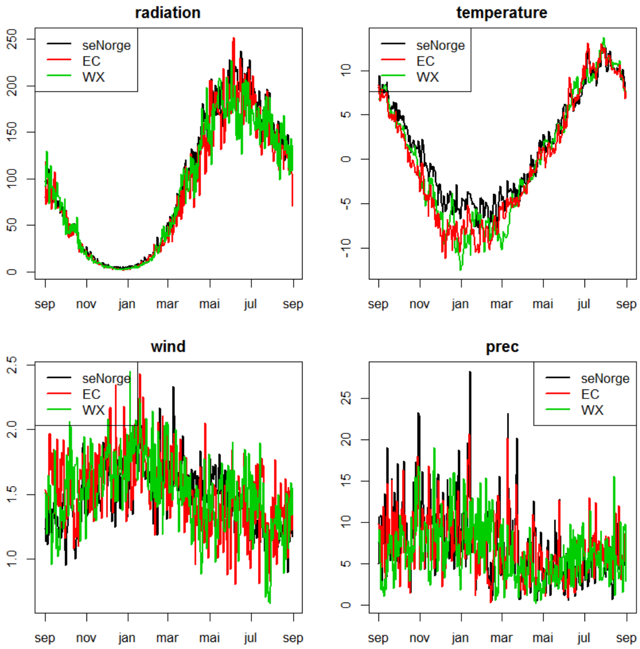

Figure 17: Yearly profile for temperature, solar radiation, wind and precipitation averaged over the Myrkdalsvatn catchment.

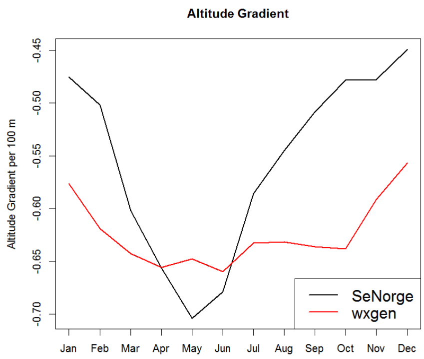

Figure 18: Seasonality in the altitude gradient as estimated from the seNorge dataset (black) and from the downscaled EC dataset (red).

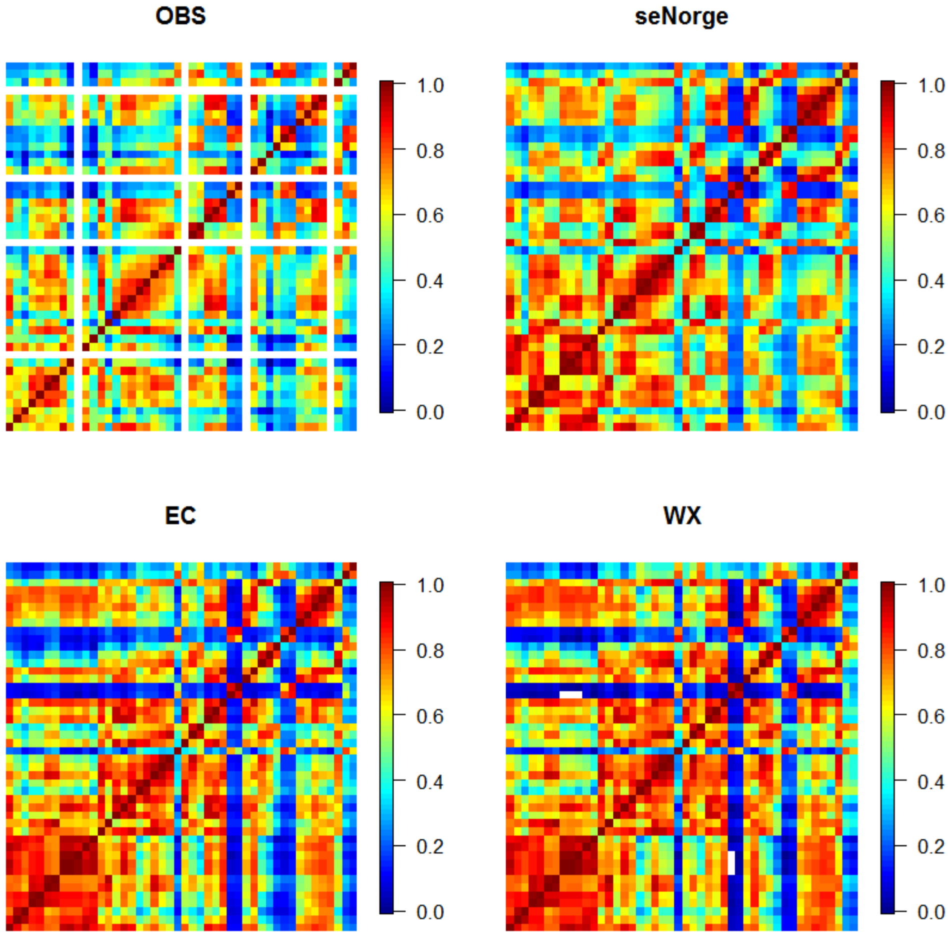

Figure 19: Matrix of daily correlation for the observed, seNorge, EC and WX inflow series.

Figure 19 the stations are ordered so that those located in the same grid of the large scale model are close to each other. The daily correlation structure between the EC and the WX series is very similar. There are differences between EC and seNorge but they are not too large. They appear, after all, to be smaller than the differences between the seNorge and the observed correlation structure. Figure 20 shows the average correlation between one stations and all the others computed from the OBS dataset against the same quantity computed from the three simulated datasets. It is clearer from this figure that EC/WX have more extreme correlations in both ends of the scale. The same quantities are plotted in space in Figure 21. Some of the catchments in the lower right corner of the domain are, on average, less correlated in the simulated data sets than in the observed one. This is more evident for the EC/WX datasets than for the seNorge one.

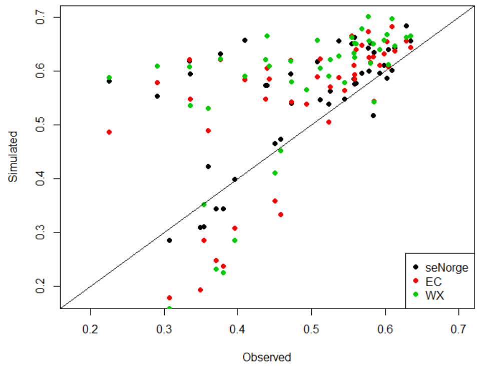

Figure 20: Average correlation between one stations and all the others computed from the OBS dataset against the same quantity computed from the three simulated datasets: seNorge (black), EC (red) and WX (blue).

The opposite happens for a group of catchments in the upper left corner. These are, on average, less correlated in the OBS data set than in the simulated ones. Again we notice that EC and WX are quite similar to each other and that the difference between EC/WX and seNorge is smaller than the difference between seNorge and OBS.

We look now at some time-aggregated data. Figure 22 shows the correlation matrix for the spring flood volume. For each inflow series we have computed the spring flood volume (April-June) and computed the linear correlation between all the stations. This estimate is based only on 10 values for each station so not too robust, but still it can give us an idea on how the *wxgen* simulator behaves when the inflow is accumulated over longer time intervals. For some catchments the EC/WX correlation appear to be negative while this is hardly the case for OBS and seNorge. Also in the positive end, EC/WX appear to have more strong correlation than OBS/seNorge.

In Figure 22 we can see differences between the EC and the WX structure. While we believe that many of the differences between the seNorge and the EC series could be mitigated by measures like better estimating the altitude gradient in the downscaling of temperature, the differences between EC and WX are due to the resampling techniques that *wxgen* uses.

5 Discussion

In this report we have presented the *wxgen* weather simulator. This is a stochastic simulator which creates multivariate synthetic weather series on a grid by resampling the output of a NWP model. *wxgen* is a flexible tool and is implemented in Python and available for testind at the website `https://github.com/metno/wxgen`. A tutorial and some guidelines are also provided in the same web site.

The ability of *wxgen* to produce realistic weather scenarios depends on the matching

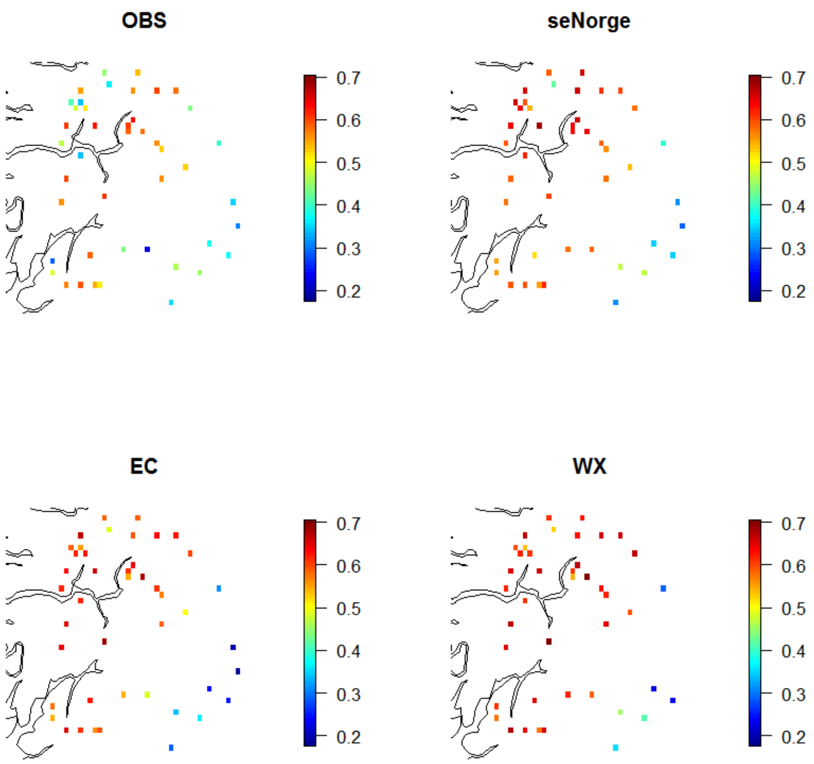

Figure 21: Average correlation between one stations and all the others computed for the four inflow datasets

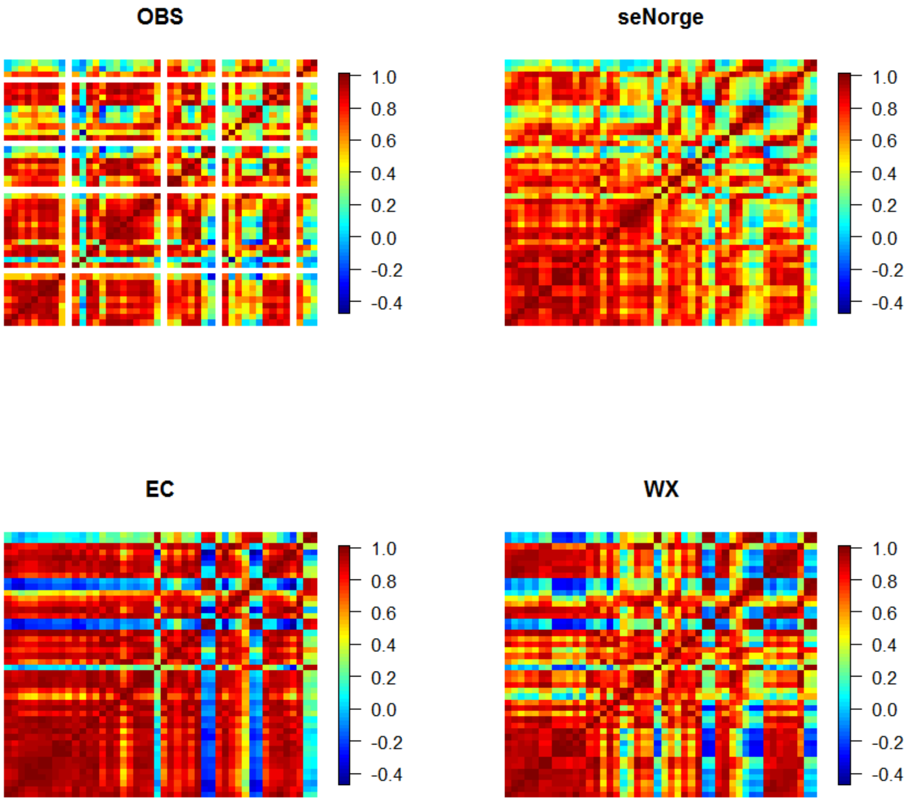

Figure 22: Correlation matrix for spring flood volume for the observed, seNorge, EC and WX inflow series.

algorithm used to join the different 10 days long weather segments and on the characteristics of the database we resample from, this, in turn depends on the characteristics of the NWP model. This means that, whatever the matching algorithm, if some bias is present in the database it will also be present in the simulated weather pattern.

In database we used in this report is a subset of the ENS-refc dataset of reforecasts maintained by the ECMWF. It consists of 10 days long weather segments on a 0.25° by 0.25° grid. The spatial domain covers the south of Norway. The database includes the following weather variables: 2 m air temperature, 10 m zonal winds, 10 m meridional winds, cloud coverage, daily totals of precipitation and sea level pressure. The precipitation and temperature variables have been corrected for drift by applying a quantile mapping between each lead time and lead time 0. The EC database presents some bias in temperature and precipitation. The precipitation bias appear to have a spatial pattern with too much precipitation in the mountains and too little on the coast but no seasonal bias. Temperature bias on the other side, has both a spatial pattern, with colder temperatures in the mountain, and a seasonal pattern, with colder and longer winters.

In this report we tested the use of a simulated weather scenario in hydrological simulation. To do this we have selected a region in central Norway with 45 observed inflow series. We have regionally calibrated a distributed hydrological model for the period 1999-2003. We have then used the calibrated parameters to simulate inflow series for 10 years. We have simulated three sets of inflow series, one using observed weather from in the period 2005-2015, the second using the day 0 forecast from the EC database also in the period 2005-2015 and the third using a 10 years long simulated weather scenario. We have then compared the simulated inflow series with each other and with the observed series.

The main difference between the observed and simulated inflow series appears to be the fact that simulated inflow series have a longer and colder winter with less activity, and a larger spring flood. This is more evident for the EC/WX data set than for the seNorge one. This is not surprising given the fact that the EC database upon which EC/WX inflows are based presents a temperature bias which makes winters longer and colder.

We have also looked at the correlation structure in the four inflow datasets. When looking at daily data, all simulated data sets appear to have somehow more extreme correlations than the observed data set. Again this is more evident for the EC/WX data sets than for the seNorge one. EC and WX data sets are very similar to each other, we only manage to notice some difference between the two data sets when looking at the correlation between spring flood volumes. Notice anyway that this correlation is based only on 10 values and its value is therefore quite unstable.

All in all, there seems to be larger similarities between the EC and WX inflow series than there are between any of OBS-seNorge, OBS-EC, OBS-WX. This indicates that the largest errors the WX inflow data set is due not to the *wxgen* simulator but to biases present in NWP model that we have used as basis for our simulator. A careful bias correction of the database (at least for the weather variables that are well observed like precipitation and temperature) might increase a lot the performance of the *wxgen* simulated weather scenarios as input for an hydrological model. Alternatively, the hydrological model can be calibrated using EC input, which is likely to build bias-correcting properties into the parameter set where achievable.

References

Buizza, R. and Leutbecher, M. (2015). The forecast skill horizon. *Quarterly Journal of the Royal Meteorological Society.*

Delle Monache, L., Nipen, T., Liu, Y., Roux, G., and Stull, R. (2011). Kalman filter and analog schemes to post-process numerical weather predictions. *Monthly weather review*, 139.

Gneiting, T. (2014). Calibration of medium-range weather forecasts. Technical report, ECMWF Technical Memorandum. `http://www.ecmwf.int/sites/default/files/elibrary/2014/9607-calibration-medium-range-weather-forecasts.pdf`.

Hamill, T. M. and Coauthors (2014). A recommended reforecast configuration for the ncep global ensemble forecast system. Technical report, NOAA White paper. `http://www.esrl.noaa.gov/psd/people/tom.hamill/White-paper-reforecast-configuration.pdf`.

Kolberg, S. and Saether, B. (2017). Operasjonalisering av fordelt tilsigsmodell i vannkraftbransjen. Technical Report 2017:00785, SINTEF Energi.

Lussana, C., Saloranta, T., Skaugen, T., Magnussson, J., Tveito, O. E., and Andersen, J. (2017a). Evaluation of senorge2, a conventional climatological datasets for snow- and hydrological modeling in norway. *Earth Syst. Sci. Data Discuss.* `https://www.w3.org/TR/owl2-overview/`.

Lussana, C., Tveito, O. E., and Uboldi, F. (2017b). Three-dimensional spatial interpolation of two-meter temperature over norway. *Quarterly Journal of the Royal Meteorological Society.* `http://dx.doi.org/10.1002/qj.3208`.

Nipen, T., Martino, S., and Lussana, C. (2017). A stochastic weather generator based on resampling historical ensemble weather forecasts. *In preparation.*

Vitart, F. and Coauthors (2017). The subseasonal to seasonal (s2s) prediction project database. *Bulletin of the American Meteorological Society,*, 98(1):163173.

Wilks, D. S. and Wilby, R. L. (1999). The weather generation game: a review of stochastic weather models. *Progress in Physical Geography*, page 329357.

Name	Serienr	Area (Km^2)	Missing (%)
Myrkdalsvatn	62.10.0	60.2	0
MIDDAL	36.9.0	46.17	57.37
Grosettjern	16.66.0	6.46	0
Bondhus	46.4.0	50.11	9.72
Brakhaug	46.7.0	9.16	77.16
Kvenna	16.140.0	818.46	9.15
Hangstjern	12.212.0	11.54	0
Fønnerdalsvatn	46.9.0	6.82	0
Feios	71.5.0	75	82.8
Bøyumselv	78.8.0	36.9	0
Byttevatn	83.6.0	103.47	0
Grønengstølsvat	83.7.0	64.33	0
Sogndalsvatn	77.3.0	111	0
Nessedalselv	79.3.0	29.8	0
Sygnesandselva	84.19.0	10.46	26.64
Sægrova	84.7.0	8.1	72.97
Lunde	84.30.0	34.22	16.65
Lovatn	88.4.0	234	0
Bulken rest	62.5.0		0
Hølen	50.1.0	228.76	0
Brekke bru	72.5.0	268	0
Reinsnosvatn	48.5.0	118.5	0
Rest Sandvenvatn	48.1.0	345.5	0
Årdalsvatn	74.1.0	190.15	0
Grunke	12.197.0	184.04	3.34
Storeskar	12.215.0	119.89	0
Vindelelv	12.207.0	269.09	0
Hølervatn	12.171.0	79.33	0
Liavatn	2.275.0	211.66	20.02
Gilja	75.22.0	205.64	0
Fornabu	74.18.0	52.93	0
Krokenelv	75.23.0	45.99	6.65
Feigumfoss	75.28.0	47.86	0
Nigardsbrevatn	76.5.0	64.87	0
Sula	73.27.0	30.31	0
Frostdalen	73.21.0	25.61	0
Brustuen	2.290.0	252.98	0
Sjodalsvatn	2.13.0	478.86	0
Akslen rest	2.268.0	539.9	0
Viertjern	16.127.0	48.86	2.96
Eggedal	12.178.0	308.69	0
Orsjøen	15.79.0	1140.55	6.65
Austbygdåi	16.128.0	294.22	0
Borgåi	15.53.0	97.54	0
Bjoreio	50.13.0	262.65	0

Table 1: Names, NVE series number and catchment area for the 46 observed inflow series

Routine	Parameter Name	Parameter Value
PristleyTaylor	LandALbedo	0.2
PristleyTaylor	PTalpha	1.26
GamSnow	TX	-0.449946*
GamSnow	WindScale1	6.91599 *
GamSnow	Windconst	0
GamSnow	MaxLWC	0.1
GamSnow	SurfaceLayer	31.7768 *
GamSnow	Maxalbedo	0.9
GamSnow	Minalbedo	0.65
GamSnow	FastDecayRate	2.1463 *
GamSnow	SlowDecayRate	16.7301 *
GamSnow	ResetSnowDepth	32.3295 *
GamSnow	GlacierAlb	0.207345*
KirchnerResponse	EvapQscale	0.0987568*
KirchnerResponse	LnTau3	5.9353 *
KirchnerResponse	DlnTauDlnQ	-0.897125*

Table 2: Routines and relative parameters included in the hydrological model. The star (*) indicates that the parameter has been calibrated.

Option	Function
-db	Database to use a basis for resampling
-v	Variables to be included in the synthetic weather scenario
-w	Weights to assign to each weather variable when computing the metric in Equation 1
- n	Number of ensemble members to simulate
-t	Length (in days) of each ensemble member
-o	Name of the output database
-wl	Level of wavelet decomposition to use when computing the metric in Equation 1

Table 3: Options for the *wxgen* generator in simulation mode used to generate the weather sequence used in this report, for more options see the wiki page of the project.